PCCP

The Effect of Dilution on Induced Free Charge Density Gradients in Room Temperature Ionic Liquids

Journal:	*Physical Chemistry Chemical Physics*
Manuscript ID	CP-ART-11-2021-005027.R1
Article Type:	Paper
Date Submitted by the Author:	05-Jan-2022
Complete List of Authors:	Hossain, Md.; Michigan State University, Department of Chemistry Blanchard, Gary; Michigan State University, Department of Chemistry

The Effect of Dilution on Induced Free Charge Density Gradients in Room Temperature Ionic Liquids

Md. Iqbal Hossain and G. J. Blanchard*
Michigan State University
Department of Chemistry
East Lansing, MI 48824 USA

Abstract

We report on changes in the magnitude and length scale of the induced free charge density gradient, ρ_f, in three imidazolium room temperature ionic liquids (RTILs) with dilution by methanol and acetonitrile. Using depth- and time-resolved fluorescence measurements of cresyl violet rotational diffusion, we find that ρ_f persists in RTILs to varying degrees depending on RTIL and diluent identity, and in all cases the functional form of ρ_f is not a smooth monotonic diminution in either magnitude or persistence length with increasing diluent, but a stepwise collapse. This finding is consistent with changes in the bulk RTIL as a function of dilution seen using rotational diffusion measurements that show the rotating entity in bulk RTILs exhibits a larger effective hydrodynamic volume than would be expected based on bulk viscosity data for the diluted RTILs. This excess hydrodynamic volume can be understood in the context of aggregation of RTIL ion pairs in the diluted RTIL system. The size of the aggregates is seen to depend on RTIL identity and diluent, and in all cases aggregate size increases with increasing dilution. This finding is consistent with the ρ_f dependence on dilution data. The collapse of ρ_f is seen to correlate with the onset of RTIL ion pair dimer formation, a condition that may facilitate dissociated RTIL ion mobility in the binary system.

* Author to whom correspondence should be addressed: email: blanchard@chemistry.msu.edu Tel: +1 517 353 1105.

Introduction

Room temperature ionic liquids (RTILs) have received a great deal of attention because of their utility in a number of applications, ranging from chemical synthesis and catalysis to chemical sensing, supercapacitors, reactive gas storage and transport, and ion propulsion.[1-6] Among the attractive properties of ionic liquids are their characteristically wide electrochemical window, extremely low vapor pressure and their ability to solubilize both polar and non-polar compounds. Despite the wide use of RTILs, this class of materials remains to be understood fully. A larger goal of our work is to improve our fundamental understanding of the structural and dynamical properties of RTILs.

In a liquid medium, thermal energy gives rise to Brownian motion of the constituent species, and an important question is precisely what the dominant species in a RTIL are. The anion and cation can exist as discrete ionic species or as a paired, dipolar moiety and the equilibrium constant for this process has been the subject of much investigation. Estimates have ranged from very little dissociation to extensive dissociation,[7-8] and several recent works have concluded that imidazolium RTILs are *ca*. 60% dissociated at room temperature.[9-10] Understanding the extent of dissociation is central to evaluating other RTIL properties, such as conductivity and dielectric response.

Recent work from our group and others has pointed to the existence of relatively long-range order in RTILs, but the details of the "order" seen by these groups remains to be connected. The Israelachvilli group reported order on the nanometer length scale based on force measurements and suggested based on that finding that the free ion concentration in RTILs was very low.[7, 11-13] The Fayer group, in a series of elegant experiments using small molecules as probes, has identified organization with a persistence length on the order of tens to hundreds of nm in RTILs,[14-19] and

the Shaw group has identified the evolution of structural order on the micrometer length scale in thin RTIL films.[20-23] Very recently, the Welton group has identified spatial variation in *n*, the refractive index, over distances of tens to hundreds of nm using Raman scattering.[24] It is clear from all these studies that RTILs exhibit structural order over length scales vastly in excess of what is typical for liquid phase solvents.

In addition to the structural order seen by the Fayer, Shaw and Welton groups, the Blanchard group has identified the existence of an induced free charge density gradient (ρ_f) in RTILs that persists over length scales on the order of 50 μm.[25-29] The free charge density gradient exists in the form of a gradient in the concentration of discrete ionic species in the RTIL, induced by the presence of a charged surface in contact with the RTIL, and sensed by either rotational diffusion[25-26] or induced birefringence[29] experiments. Not only does the length scale of this gradient differ from the organization seen by others, but the charge density gradient does not necessarily correspond to a structural gradient. It is of fundamental interest to determine how local and longer-range organization in RTILs is related to the induced free charge density gradient. In the work presented here one focus is on the effect of dilution on ρ_f, which is seen to collapse upon the addition of 20 to 30 mol% of diluent. We also report that, as a result of this finding, we have identified the existence of molecular-scale aggregates in RTIL solutions of acetonitrile (ACN) and methanol, even at high dilution, well beyond the point where ρ_f is no longer seen. These distinct and complementary findings suggest the existence of persistent compositional heterogeneity in diluted RTIL systems. The RTILs we have chosen for this work are $BMIM^+BF_4^-$, $BMIM^+TFSI^-$ and $HMIM^+TFSI^-$ in order to gauge the importance of cation and anion identity, and for the characterization of ρ_f we have used the cationic chromophore cresyl violet (CV^+). The structures of these compounds are shown in Fig. 1. The data we report for these systems provide insight into

the short-range organization in RTILs and the relationship of this organization to the longer-range charge density gradient.

Experimental Section

Chemicals. $BMIM^+BF_4^-$ (≥ 97.0%), $BMIM^+TFSI^-$ (≥ 99%, H_2O <500 ppm) and $HMIM^+TFSI^-$ (≥ 98%, Sigma-Aldrich) were used after purification (*vide infra*). Acetonitrile (anhydrous, 99.8%, ~50 ppm H_2O) and methanol (anhydrous, 99.8%, ~50 ppm H_2O) were purchased from Sigma-Aldrich, dried over activated 4 Å molecular sieves and stored inside a dry box (glove box). Cresyl Violet perchlorate (Eastman Kodak Co.), ethanol (≥ 99.5%, Sigma-Aldrich), activated charcoal (powder, −100 particle size, Sigma-Aldrich), and isopropyl alcohol (≥ 99.5%, Macron Fine Chemicals) were used without further purification. Water used in these studies was purified with a Milli-Q filtration system (Millipore). ITO coated glass slides (Nanocs Inc., IT10-111-25, 10 Ω/sq) and silicone rubber sheet of 1 mm thickness (MSC Direct) were needed to prepare the cell spacer as described below.

Purification of ILs. As-received RTILs $BMIM^+BF_4^-$, $BMIM^+TFSI^-$ and $HMIM^+TFSI^-$ were stored over activated carbon for at least two weeks. After this time, the activated carbon powder has been removed from RTILs using a syringe filter (Durapore membrane, 0.22 μm sterile filtration, Millex). Next, the RTILs are heated to 85 °C for five hours while purging with ultrapure Argon (99.9995%, Linde). The procedure was performed with the RTILs in a round bottom flask on a N_2-purged Schlenk line. The water content in the RTILs was measured Karl Fischer titration (Mettler Toledo C10SD) and found to be ≤ 45 ppm). The purified RTILs are then stored in a dry glove box until they are used in experiments.

Preparation of RTIL-Chromophore Solution. Stock solution of chromophore (*ca*. 5.34 x 10^{-4} M) in ethanol was prepared. The chromophore (final concentration of 5.34 x 10^{-5} M) + RTILs

solution was prepared by dispensing 100 μL of the chromophore stock solution (30 minutes sonication prior to use) using an Eppendorf pipette into a scintillation vial, followed by 3 h at 100 °C to evaporate the ethanol. The vial was then cooled in a desiccator. An aliquot of 1 mL of purified RTIL was transferred by Eppendorf pipette to the vial. This stock solution was then stirred for at least 12 h before use. All glassware was stored in an oven at 150 °C for at least 24 h before use to minimize water contamination. All sample preparation procedures were performed in a N_2-purged vinyl dry box (Coy Laboratories, Grass Lake, MI). The water vapor in the box was ≤ 5 ppm, as measured with a hygrometer.

Sample Cell Preparation. The sample cell used in this work has been described elsewhere.[26] Briefly, ITO coated supports were cleaned by sonication in a detergent solution, then Milli-Q water, and isopropanol for 15 min each. ITO was used because it carries a net positive surface charge.[30] No current or voltage was applied to either support in the work we report here.[26] After that the supports were washed with ethanol (200 proof, anhydrous) and dried in an oven at 200 °C for 40 mins. After cooling by purging nitrogen, a UV/ozone cleaner was used to clean the supports for 20 min. The cell spacer (1.6 mm) was cut from a silicone rubber sheet, washed by sonication in detergent solution, and in Milli-Q water, and then dried with flowing N_2 for 15 min each.

Fluorescence Anisotropy Decay Measurements. The TCSPC imaging instrument used in this work has been described in detail elsewhere.[31] The system is the combination of a time correlated single photon counting (TCSPC) laser system coupled with an inverted confocal laser scanning microscope (Nikon Eclipse Ti-U) which provides 1.2 μm depth resolution with a 10X objective (N.A. 0.30). The light source is a synchronously pumped, cavity dumped dye laser (Coherent 701-3) excited by the second harmonic output of a passively mode locked Nd: YVO_4 laser. The output of the dye laser is *ca*. 5 ps pulses at a repetition rate of 4 MHz. The TCSPC electronics (Becker

& Hickl SPC-152) are used to acquire polarized emission transients. Time resolution is limited by the avalanche photodiode detectors (ID Quantique) to *ca*. 100 ps. Signal averaging in the plane of detection is performed by acquisition of time-resolved data over a region of the sample at a pre-determined depth using a confocal scanning head (Beck & Hickl DCS-120). Mechanical control over microscope stage vertical position provides spatial (depth) resolution for the time-resolved anisotropy decay measurements. Primary depth-dependent reorientation data are provided in the Supporting Information. Uncertainties in the primary data are the standard deviations of fitted time constants for 65,536 sets of time-resolved data (256 x 256 array) and uncertainties in derived quantities are propagated from uncertainties in the primary data.

Binary Systems Preparation. Binary RTIL/solvent systems were prepared by mass. We mixed measured masses of each component for a given RTIL/solvent system and from that information calculated the mole fraction volumetrically (v/v)%. To minimize water contamination, all binary systems were prepared in a N_2-purged vinyl dry box (Coy Laboratories, Grass Lake, MI). Sealed samples were maintained in the dry box until measurements were performed.

Results and Discussion

As indicated in the Introduction, there are two related issues we address in this work. The first is the effect of dilution on the induced free charge density gradient seen in RTILs and the second is the role of compositional (spatial) heterogeneity in RTILs that have been diluted. In particular, we are interested in the characteristic differences in the role of hydrogen bonding in diluted RTIL systems and for that reason we report on the effect of dilution of RTILs with protic (methanol) and aprotic (acetonitrile) solvents. In the discussion that follows, we briefly recap the properties of the induced free charge density gradient seen in RTILs and discuss the manner in which we probe the effects of dilution of RTILs prior to consideration of the specific results.

The Blanchard group has reported on the ability of a charged surface in contact with a RTIL to induce a free charge density gradient, ρ_f.[25-29] The gradient was initially identified through the dependence of the rotational diffusion time constant, τ_{OR}, of a charged chromophore in the RTIL on the distance from the charged support. The gradient in the density of charged (dissociated) species in the RTIL produces a corresponding gradient in the amount of free and complexed chromophore, and thus a gradient in the average volume of the reorienting entity. The spatial extent of ρ_f has been shown to be *ca*. 50 μm (e^{-1} depth). The magnitude of the gradient can be inferred from the normalized change in τ_{OR} with distance from the charged surface and it depends on the identity of the RTIL constituent species.[27] The quantity ρ_f is related to a gradient in the dielectric response of the RTIL and through control of the surface charge, σ_s, on the RTIL support surface, a gradient in the real part of the RTIL complex refractive index can be characterized.[29] Such an induced birefringence is not only important for potential applications, but it also provides a way to characterize ρ_f without the addition of a chromophore to the RTIL. Despite the characterization of ρ_f we have reported to date, a full understanding of the fundamental RTIL properties that support the existence of ρ_f over macroscopic distances remains to be achieved.

Several factors are required to support ρ_f over macroscopic distances, including effective charge screening and limited charge mobility. While the extent of RTIL dissociation is not known with great certainty, a body of work points to these species being *ca*. 60% dissociated at room temperature.[9-10] In an effort to understand the relative importance of ionic (charge) mobility in maintaining ρ_f, it is instructive to compare the results for neat RTILs to the known result in the dilute solution limit (the electric double layer) and to characterize the effect of RTIL dilution on the persistence length and magnitude of ρ_f.

It has been reported previously that the interactions between solvents and RTIL constituents differ significantly, *i.e.* RTIL anions and cations experience different interactions with diluting solvents,[9, 32] and this is not surprising. Further, the role of hydrogen-bonding interactions between protic solvents and RTIL anions such as BF_4^- are thought to facilitate mobility of the anion.[9, 32] Based on these findings it is reasonable to expect dilution to exhibit a significant effect on the persistence length and magnitude of ρ_f. To test this hypothesis, we have studied the rotational diffusion dynamics of the cationic chromophore cresyl violet (CV^+) as a function of distance from a charged support surface and as a function of RTIL and dilution with solvents acetonitrile (polar aprotic solvent) and methanol (polar protic solvent). Our findings demonstrate that ρ_f can withstand significant dilution before ceasing to exist, and that the RTIL/solvent binary systems are not homogeneous, even at comparatively high dilutions. We discuss these findings separately.

The information we acquire is in the form of the dependence of the chromophore rotational diffusion time constant on distance from a charged support surface. The experimental data are polarized time-domain emission decays, taken at polarizations parallel and perpendicular to the excitation polarization, $I_{\parallel}(t)$ and $I_{\perp}(t)$. The difference between these polarized decays, normalized for fluorescence lifetime, is the anisotropy decay function, R(t) (Eq. 1),

$$R(t) = \frac{I_{\parallel}(t) - I_{\perp}(t)}{I_{\parallel}(t) + 2I_{\perp}(t)} \qquad [1]$$

The functional form of R(t) provides chemically and physically useful information. For all the measurements we report here, R(t) decays as a single exponential with a time constant τ_{OR}, the orientational relaxation time. The quantity τ_{OR} is related to the viscosity of the medium (η) and the volume of the reorienting entity (V) through the Debye-Stokes-Einstein equation (Eq. 2).[33-35]

$$\tau_{OR} = 6D_{rot}^{-1} = \frac{\eta V f}{k_B T S} \quad [2]$$

Where D_{rot} is the rotational diffusion constant, f is a frictional interaction term and S is a shape factor to account for ellipticity of the rotating entity.[33-35] For polar and ionic species $f = 1$ and S depends slightly on whether the rotating entity is the free or complexed chromophore and in all cases is close to 1.[34-35] From earlier work we have shown that the depth-dependent change in τ_{OR} is related to the depth-dependent change in the average volume of the reorienting entity, V_{eff},[25]

$$V_{eff} = X_{dissociated} V_{dissociated} + X_{associated} V_{associated} \quad [3]$$

The relevant equilibrium is

$$CV^+ + A^-_{RTIL} \rightleftharpoons (CVA_{RTIL}) \quad [4]$$

With CV^+ being the dissociated chromophore and CVA_{RTIL} being the associated species. The hydrodynamic volumes of CV^+ and A^-_{RTIL} (the RTIL anion) are calculated using the method of Van der Waals increments[36] and $X_{dissociated} + X_{associated} = 1$. The variation in V_{eff} with distance from the charged support surface is given by Eq. 5,

$$\nabla V_{eff} = \nabla X_{dissociated} V_{dissociated} + \nabla X_{associated} V_{associated} \quad [5]$$

Which is related to the reorientation time gradient (Eq. 6),

$$\nabla \tau_{OR} = \frac{\eta f}{k_B T S} \nabla V_{eff} \quad [6]$$

The gradient in V_{eff} is due to the gradient in $[A^-_{RTIL}]$ which represents a gradient in the displaced charge ($Ð$) in the system (Eq. 7),[25]

$$\nabla \tau_{OR} = k \nabla \cdot Ð = k \rho_f \quad [7]$$

Where k is a proportionality constant, and ρ_f is the free charge density gradient in the RTIL. Because τ_{OR} varies with the identity of the RTIL and the chromophore used, it is important to

present data for such measurements in a manner that can be compared across RTILs and in a chromophore-independent manner. We report the normalized gradient in τ_{OR} as[27]

$$\left(\frac{\Delta\tau_{OR}}{\tau_{OR}}\right)(x)=\frac{\left(\tau_{OR}^{x}-\tau_{OR}^{\infty}\right)}{\tau_{OR}^{\infty}}=\left(\frac{\Delta\tau_{OR}}{\tau_{OR}}\right)(0)\exp(-x/d) \qquad [8]$$

Where x is the axis perpendicular to the support surface plane and d is the e^{-1} persistence length of ρ_f. The quantity τ_{OR}^{x} is the orientational relaxation time at distance x from the support surface and τ_{OR}^{∞} is the orientational relaxation time at distances sufficiently far from the charged support that $\rho_f = 0$. It is the dependence of the quantities $(\Delta\tau_{OR}/\tau_{OR})(0)$ and d on dilution that are of interest. We fit the experimental data using least squares fitting to obtain values of $(\Delta\tau_{OR}/\tau_{OR})(0)$ and d. The quantity $(\Delta\tau_{OR}/\tau_{OR})(0)$ is a gauge of the magnitude of ρ_f and d is a measure of the persistence length of ρ_f, and the dependence of each of these quantities on the amount and identity of diluent added to the RTIL reflects the extent to which these binary systems behave as homogeneous media.

We show the dependence of $(\Delta\tau_{OR}/\tau_{OR})(0)$ (panels a and b) and d (panels c and d) on dilution for the RTILs $BMIM^{+}BF_4^{-}$, $BMIM^{+}TFSI^{-}$ and $HMIM^{+}TFSI^{-}$ with acetonitrile and methanol, in Figs. 2, 3 and 4, respectively. These data contain several significant features. The first is that the magnitude of ρ_f depends on the extent of dilution, but this dependence is not a smooth trend with increasing dilution. Rather, ρ_f remains at a relatively constant level with increasing dilution up to a point and then diminishes to 0 with slight additional dilution. The trend is similar for all the RTILs examined and there is a noticeable difference in the dilution at which ρ_f ceases to persist in acetonitrile and methanol. Both the functional form of the data and the amount of solvent required to cause ρ_f to collapse are consistent with the binary system being spatially heterogeneous. The basis for this assertion is the known monotonic dependence of RTIL-solvent system viscosity on solvent concentration.[37-40] In a homogeneous system, ion mobility is

inversely proportional to viscosity, leading to the prediction that ρ_f should diminish in proportion to the reduction in viscosity, a prediction that is at odds with the functional form of the ρ_f data in Figs. 2-4. By way of comparison, the viscosities for which ρ_f is seen to vanish is on the order of 20 cP with acetonitrile dilution and 40 cP with methanol dilution for $BMIM^+BF_4^-$. Normal solvents, such as ethylene glycol (15 cP)[41] or even higher viscosity solvents such as glycerol (1400 cP)[42] do not support free charge density gradients. Ion mobility thus appears not to be the primary factor leading to the loss of ρ_f with dilution.

The dependence of d on dilution is also shown in Figs. 2-4 (panels c and d), and it does not depend smoothly on dilution. Rather, d is seen to correlate closely with $(\Delta\tau_{OR}/\tau_{OR})(0)$. This information is also consistent with the notion that the RTIL/solvent binary system is not homogeneous, even to significant levels of dilution. The magnitude and spatial extent of ρ_f both appear to change little with dilution until a critical point is reached and the binary RTIL/solvent system will no longer support the charge density gradient. This critical point differs for the two solvents; in acetonitrile, all RTILs exhibit this change in ρ_f and d for X_{ACN} between 0.3 and 0.4, and for X_{MeOH} between 0.2 and 0.25. In addition to the implication that the RTIL/binary solvent system is not uniform, even for relatively high dilution, our findings also suggest that the organization of these binary systems serves to screen ionic charge very effectively.

As noted above, the dependence of bulk viscosity on RTIL/solvent binary system composition has been reported and varies smoothly with extent of dilution.[37-40, 43-46] It is important to consider that the measurement of bulk viscosity represents an average of intermolecular interaction energies over poorly-defined macroscopic length scales. Specifically, the viscosity is a measure of the frictional interactions between the species that are present in the liquid and, while it is typically taken as representing intermolecular interactions in liquids, this assumption is not

necessarily correct in complex multi-component systems. We have examined the rotational diffusion dynamics of CV^+ in the RTILs shown in Fig. 1 at a depth within the sample (> 100 μm) where ρ_f is seen to have no effect, as a function of dilution with acetonitrile and methanol. The purpose of this work is to compare the effective viscosity sensed by CV^+, which is inherently on a molecular length scale, to the known bulk viscosities of the RTILs as a function of dilution.

The Debye-Stokes-Einstein equation (Eq. 2) relates the induced orientational anisotropy decay time constant to the thermal energy of the system (k_BT), parameters that relate to the volume and shape of the rotating entity (V and S) and the interactions between the rotating entity and the surrounding medium (η and f). Implicit in this model is that the medium surrounding the rotating entity behaves as a continuum and this approximation is valid when the volume of the rotating species is much larger than the volume of the individual (solvent) molecules surrounding it.[33-35] Experimentally this approximation is seen to hold reasonably well in polar systems where the reorienting species and the solvent are similar in size.[47-48] The use of η carries with it the approximation that the intermolecular interactions between solvent molecules are the same as those between the solvent and the rotating entity. This approximation is typically valid and if there is any difference between solvent-solvent and solvent-solute interactions, that difference is constant for all measurements in a given series where solute concentration, for example, is varied.

The relationship between RTIL dilution and bulk viscosity has been reported before for a number of systems, including the ones considered in this work.[32, 37, 39-40, 49-51] Characteristically, there is a smooth, monotonic dependence of the measured bulk viscosity and amount of diluent added. We can use these data in concert with the hydrodynamic volume of CV^+ (217 $Å^3$)[25, 36] to calculate the reorientation time constants as a function of RTIL dilution using Eq. 2. For a homogeneous system, where the reorienting entity is the CV^+ chromophore, the experimental

dependence of τ_{OR} on solvent dilution should match the predictions of Eq. 2, save perhaps for a small scaling factor, but in any event the functional form of the experimental data and that predicted by Eq. 2 should agree. We do not observe this agreement experimentally. We show in Figs. 5 the calculated vs. experimental reorientation times for CV^+ in the RTILs as a function of dilution with acetonitrile (left) and methanol (right).

The data contained in Figs. 5 could be interpreted in several ways. Based on Eq. 2, one potential reason for the deviation between experimental and predicted time constants could be that the intermolecular interactions between CV^+ and the molecules in its immediate vicinity differ energetically from interactions between two constituent species in the RTIL. Such a difference could also be viewed as a variation in the frictional term, *f*, with dilution. There is an interesting body of work that shows the nature of solvent-solute coupling can exhibit heterogeneity in complex systems,[52-53] but we believe that such heterogeneity is not dominant in the systems under consideration because the timescale of environmental exchange that would give rise to such an effect would be necessarily much shorter than the measured rotational diffusion times reported here. In other words, any short-term fluctuations in *f* would be temporally averaged over the timescale relevant for chromophore rotation. Another possible explanation could be in the context of a change in *S* with dilution, but as noted above, there is insufficient possible variation in the value of *S* ($0.75 < S < 1$) to account for these findings.[35] For these reasons, we believe the most plausible explanation for these findings is that the volume of the reorienting entity is changing with dilution and, in all cases, the volume of the reorienting entity is larger than the hydrodynamic volume of CV^+. Indeed, we have found this to be the case in terms of explaining the basis for the observed ρ_f in RTILs and assume changes in the hydrodynamic volume of the reorienting entity accounts for the results we report here.

It is well established that the rotational diffusion of polar chromophores in polar liquids are consistent with the calculated hydrodynamic volume of the chromophore is in good agreement with experimental data.[47-48, 54] For reorientation in RTILs, this is not the case, and these data are consistent with the RTIL/solvent system being spatially heterogeneous even under conditions of relatively high dilution. There is literature precedent and support for this assertion[44, 46, 55-57] and the issue is how to model the reorienting entity. It is possible, in principle, to account for the hydrodynamic volume in excess of that for CV^+ to be accounted for either as solvent aggregates in the RTIL or RTIL aggregates in the diluent. There is literature precedent for solvent-RTIL interactions that has demonstrated clusters of RTIL ion-pairs in the solvent medium[44-46, 55] and we evaluate the data shown in Figs. 5 in that context. The hypothesis is that the CV^+ chromophore is interacting primarily with the RTIL ion-paired clusters in the binary solvent system and the rotational diffusion time constants reflect the motion of the chromophore-RTIL complex. The hydrodynamic volumes of the RTIL constituents are provided in Table 1. The effective volume of the rotating entity can be used to estimate into the average number of RTIL ion-paired complexes interacting with the chromophore as a function of dilution (Fig. 6). In Fig. 6 the blue lines indicate the hydrodynamic volumes of the (ion-paired) chromophore plus integer numbers of RTIL ion pairs. There are several significant features contained in these data.

In considering the data shown in Fig. 6, indicating the effective rotor volume vs. mole fraction of diluent added, it is important to note that the reorientation time constant values do not necessarily need to coincide with the volume of the rotor and an integral number of RTIL ion pairs. Non-integer values of RTIL ion pairs correspond to the average lifetime of the complex being less than the rotational diffusion time constant. The data in Fig. 6 show that the number of RTIL ion-pairs complexed to the chromophore appears to increase with increasing solvent dilution. The

extent of the effect depends sensitively on the RTIL identity and to a lesser extent on diluent concentration, indicating in all cases an increase in aggregate size with increasing dilution. The dependence on RTIL identity for each diluent shows that aggregation is more pronounced with up to 12 RTIL ion pairs involved in aggregation with the chromophore for $BMIM^+BF_4^-$ in acetonitrile at high dilution, approximately 5 RTIL ion pairs for $BMIM^+TFSI^-$ and something closer to dimer formation at *ca*. 40% acetonitrile with $HMIM^+TFSI^-$. We note that for $BMIM^+TFSI^-$ at the same dilution, we observe the same dimer-like formation. Based on these findings, it appears that the RTIL anion and how the diluent interacts with it plays a deterministic role in the aggregate formation we observe, and the RTIL cation is less affected by the type or amount of diluent. The same qualitative trends are seen with methanol as the diluent, allowing no clear distinction between dipolar solvent-RTIL interactions and hydrogen-bonding solvent-RTIL interactions based on these data. While there has been some consideration in the literature for the relative importance of dipolar solvation and hydrogen-bonding interactions in RTIL dilution studies, the data we report here do not show a discernible distinction between these two very distinct molecular interactions. What is clear, however, is that the dilution of the imidazolium RTILs we have studied here leads to the formation of aggregates in the binary system. Dilution does not produce a homogeneous solution, at least to the extent we have diluted the RTILs. We can therefore not make a direct connection to dilute solution limit behavior of aqueous salt solutions for RTILs.

The collapse of the induced free charge density gradient ρ_f with dilution correlates with onset of aggregation between the chromophore and RTIL ion pairs seen in the bulk RTILs. The gradient ρ_f is seen to collapse when dimer-like species are found in the bulk diluted RTILs (*i.e.* $V(CV^+A^-) + 1V(RTIL)$). The structural heterogeneity afforded by the formation of aggregated species may facilitate the mobility of dissociated RTIL ions in the solvent-rich regions of the

heterogeneous system, leading to the inability of the system to support ρ_f. Further work is required to understand the relationship between the collapse of ρ_f the formation of dimers and higher multimers in diluted RTIL systems.

Conclusions

We have examined the dependence of the magnitude and persistence length of ρ_f in three imidazolium RTILs on dilution with polar protic and aprotic solvents methanol and acetonitrile. We find that ρ_f persists in RTILs to varying degrees depending on RTIL and diluent identity, and in all cases the functional form of ρ_f is not a smooth, monotonic diminution with increasing diluent, but rather a stepwise change. This finding is not consistent with dilution producing a homogeneous solution. An examination of changes in the bulk RTIL as a function of dilution using rotational diffusion measurements shows that the rotating entity in bulk RTILs exhibits a larger effective hydrodynamic volume than would be expected based on bulk viscosity data for the diluted RTILs. This excess hydrodynamic volume is understood in the context of aggregation of RTIL ion pairs in the diluted RTIL system. The size of the aggregates is seen to depend on RTIL identity and diluent, and in all cases aggregate size increases with increasing dilution. This finding is consistent with the ρ_f dependence on dilution data. The collapse of ρ_f is seen to correlate with the onset of RTIL ion pair dimer formation, a condition that may facilitate dissociated RTIL ion mobility in the binary system. Further work on selected solvent systems will likely provide greater insight into the compositional heterogeneity in RTIL-solvent binary systems.

Acknowledgment

The research was carried out under the framework of project #W911-NF-14-10063 funded by the Army Research Office.

Author Contributions

Both authors contributed to data acquisition, analysis and interpretation.

Table 1. Hydrodynamic volumes of RTIL cations and anions and CV^+. Volumes calculated using the method of van der Waals increments (Ref. [36])

Molecule	**V (Å^3)**
CV^+	217
$BMIM^+$	139
$HMIM^+$	173
BF_4^-	50
$TFSI^-$	169

References

1. C. Arbizzani; M. Biso; D. Cericola; M. Lazzari; F. Soavi; M. Mastragostino, *J. Pwr. Sources* **2008,** *185*, 1575 - 1579.

2. D. R. MacFarlane; N. Tachikawa; M. Forsyth; J. M. Pringle; P. C. Howlett; G. D. Elliott; J. H. Davis; WatanabeM.; P. Simon; C. A. Angell, *Energ. Env. Sci.* **2014,** *7*, 232 - 250.

3. J. A. Nabity; J. W. Daily, *Journal of Propulsion and Power* **2017,** *34(1)*, 260-266.

4. R. Newell; J. Faure-Vincent; B. Iliev; T. Schubert; D. Aradilla, *Electrochim. Acta.* **2018,** *267*, 15 - 19.

5. H. Sakaebe; H. Matsumoto, *Electrochem. Commun.* **2003,** *5*, 594 - 598.

6. K. L. Van Aken; M. Beidaghi; Y. Gogotsi, *Angew. Chem.* **2015,** *127*, 4888 - 4891.

7. M. A. Gebbie; M. Valtiner; X. Banquy; E. T. Fox; W. A. Henderson; J. N. Israelachvili, *Proc. Nat. Acad. Sci. USA* **2013,** *110*, 9674-9679.

8. D. R. MacFarlane; M. Forsyth; E. I. Izgorodina; A. P. Abbott; G. Annat; K. Fraser, *Phys. Chem. Chem. Phys.* **2009,** *11*, 4962-4967.

9. O. Nordness; J. F. Brennecke, *Chem. Rev.* **2020,** *120*, 12873-12902.

10. Y.-J. Lin; N. Hossain; C.-C. Chen, *J. Mol. Liq.* **2021,** *329*, 115524.

11. M. A. Gebbie; H. A. Dobbs; M. Valtiner; J. N. Israelachvili, *P Natl Acad Sci USA* **2015,** *112*, 7432-7437.

12. M. A. Gebbie; A. M. Smith; H. A. Dobbs; A. A. Lee; G. G. Warr; X. Banquy; M. Valtiner; M. W. Rutland; J. N. Israelachvili; S. Perkin; R. Atkin, *Chem. Commun.* **2017,** *53*, 1214-1224.

13. J. N. Israelachvili; Y. Min; M. Akbulut; A. Alig; G. Carver; W. Greene; K. Kristiansen; E. Meyer; N. Pesika; K. Rosenberg; H. Zeng, *Rep. Prog. Phys.* **2010,** *73*, 036601.

14. J. Nishida; J. P. Breen; B. Wu; M. D. Fayer, *ACS Cent. Sci.* **2018,** *4*, 1065-1073.

15. J. Y. Shin; S. A. Yamada; M. D. Fayer, *J. Am. Chem. Soc.* **2017,** *139*, 311-323.

16. J. Y. Shin; S. A. Yamada; M. D. Fayer, *J. Am. Chem. Soc.* **2017,** *139*, 11222-11232.

17. J. E. Thomaz; H. E. Bailey; M. D. Fayer, *J. Chem. Phys.* **2017,** *147*, 194502 1-11.

18. B. Wu; J. P. Breen; M. D. Fayer, *J. Phys. Chem. C* **2020,** *124*, 4179-4189.

19. B. Wu; J. P. Breen; X. Xing; M. D. Fayer, *J. Am. Chem. Soc.* **2020,** *142*, 9482-9492.

20. Anaredy; R. S.; S. K. Shaw, *J. Phys. Chem. C* **2018,** *122*, 19731-19737.

21. R. S. Anaredy; S. K. Shaw, *Langmuir* **2016,** *32*, 5147-5154.

22. A. J. Lucio; S. K. Shaw; J. Zhang; A. M. Bond, *J. Phys. Chem. C* **2017,** *121*, 12136-12147.

23. R. S. Anaredy; S. K. Shaw, *J. Phys. Chem. C* **2019,** *123*, 8975-8982.

24. S. Toda; R. Clark; T. Welton; S. Shigeto, *Langmuir* **2021,** *37*, 5193-5201.

25. K. Ma; R. Jarosova; G. M. Swain; G. J. Blanchard, *Langmuir* **2016,** *32*, 9507-9512.

26. K. Ma; R. Jarosova; G. M. Swain; G. J. Blanchard, *J. Phys. Chem. C* **2018,** *122*, 7361-7367.

27. Y. Wang; R. Jarosova; G. M. Swain; G. J. Blanchard, *Langmuir* **2020,** *36*, 3038-3045.

28. Y. Wang; F. Parvis; M. I. Hossain; K. Ma; R. Jarosova; G. M. Swain; G. J. Blanchard, *Langmuir* **2021,** *37*, 605-615.

29. Y. Wang; G. M. Swain; G. J. Blanchard, *J. Phys. Chem. B* **2021,** *125*, 950-955.

30. T. A. N. Peiris; S. Senthilarasu; K. G. U. Wijayantha, *J. Phys. Chem. C* **2011,** *116*, 1211-1218.

31. C. E. Hay; F. Marken; G. J. Blanchard, *Langmuir* **2014,** *30*, 9951-9961.

32. W. Li; Z. Zhang; B. Han; S. Hu; Y. Xie; G. Yang, *J. Phys. Chem. B* **2007,** *111*, 6452-6456.

33. P. Debye, *Polar Molecules* Chemical Catalog Co.: New York 1929; p 84.

34. C.-M. Hu; R. Zwanzig, *J. Chem. Phys.* **1974,** *60(11)*, 4354-4357.

35. F. Perrin, *J. Phys. Radium* **1934,** *5*, 497.

36. J. T. Edward, *J. Chem. Ed.* **1970,** *47*, 261-270.

37. E. Herold; M. Strauch; D. Michalik; A. Appelhagen; R. Ludwig, *ChemPhysChem* **2014,** *15*, 3040-3048.

38. C. Schutter; A. Bothe; A. Balducci, *Electrochim. Acta* **2020,** *331*, 135421.

39. E. Vercher; F. J. Llopis; V. Gonzalez-Alfaro; P. J. Miguel; V. Orchilles; A. Martinez-Andreu, *J. Chem. Thermodyn.* **2015,** *90*, 174-184.

40. J. Wang; Y. Tian; Y. Zhao; K. Zhuo, *Green Chemistry* **2003,** *5*, 618-622.

41. F. S. Jerome; J. T. Tseng; L. T. Fan, *J. Chem. Eng. Data* **1968,** *13*, 496.

42. J. B. Segur; H. E. Oberstar, *Ind. Eng. Chem.* **1951,** *43*, 2117-2120.

43. M. Bester-Rogac; J. Hunger; A. Stoppa; R. Buchner, *J. Chem. Eng. Data* **2010,** *55*, 1799-1803.

44. Y.-Z. Zheng; Y. Zhou; G. Deng; R. Guo; D.-F. Chen, *Spectrochim. Acta A: Mol. Biomol.Spectr.* **2019,** *223*, 117312.

45. M. Bester-Rogac; A. Stoppa; R. Buchner, *J. Phys. Chem. B* **2014,** *118*, 1426-1435.

46. Y.-Z. Zheng; N.-N. Want; J.-J. Luo; Y. Zhou; Z.-W. Yu, *Phys. Chem. Chem. Phys.* **2013,** *15*, 18055-18064.

47. G. J. Blanchard, *J. Phys. Chem.* **1988,** *92*, 6303-6307.

48. G. J. Blanchard; C. A. Cihal, *J. Phys. Chem.* **1988,** *92*, 5950-5954.

49. J. N. A. Canongia Lopes; M. F. Costa Gomes; P. Husson; A. A. H. Padua; L. P. N. Rebelo; S. Sarraute; M. Tariq, *J. Phys. Chem. B* **2011,** *115*, 6088-6099.

50. A. Zhu; J. Wang; L. Han; M. Fan, *Chem. Eng. J.* **2009,** *147*, 27-35.

51. R. Salinas; J. Pla-Franco; E. Lladosa; J. B. Monton, *J. Chem. Eng. Data* **2015,** *60*, 525-540.

52. S. Pronk; E. Lindahl; P. M. Kasson, *Nature Communications* **2014,** *5(1)*, 3034.

53. N. Das; P. Sen, *Physical Chemistry Chemical Physics* **2021,** *23(29)*, 15749-15757.

54. G. J. Blanchard, *J. Phys. Chem.* **1991,** *95*, 5293-5299.

55. B. A. Marekha; O. N. Kalugin; M. Bria; R. Buchner; A. Idrissi, *J. Phys. Chem. B* **2014,** *118*, 5509-5517.

56. N. T. Scharf; A. Stark; M. M. Hoffmann, *J. Phys. Chem. B* **2012,** *116*, 11488-11497.

57. X. Hu; Q. Lin; J. Gao; Y. Wu; Z. Zhang, *Chem. Phys. Lett.* **2011,** *516*, 35-39.

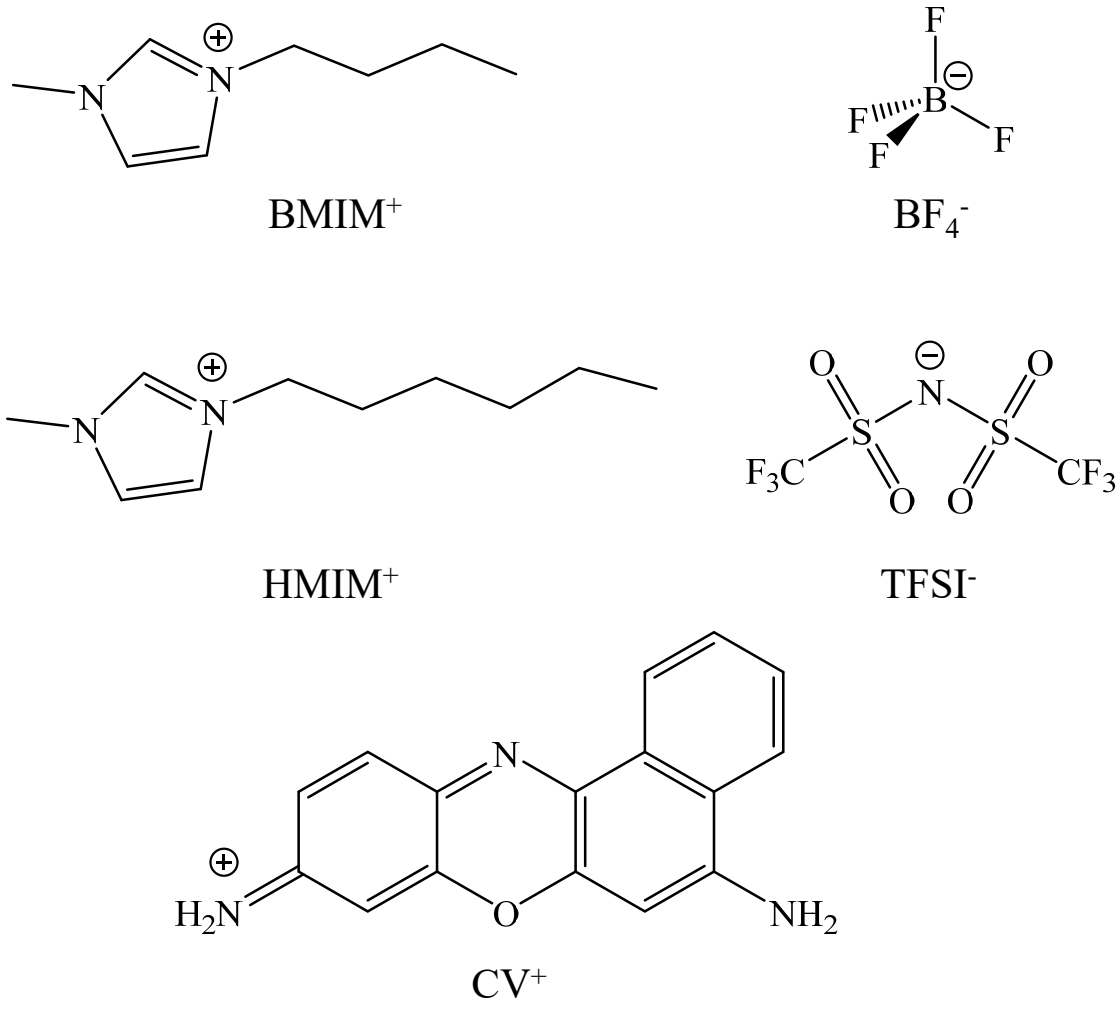

Figure 1. Structures of the RTIL cations and anions, and the chromophore cresyl violet, used in this work.

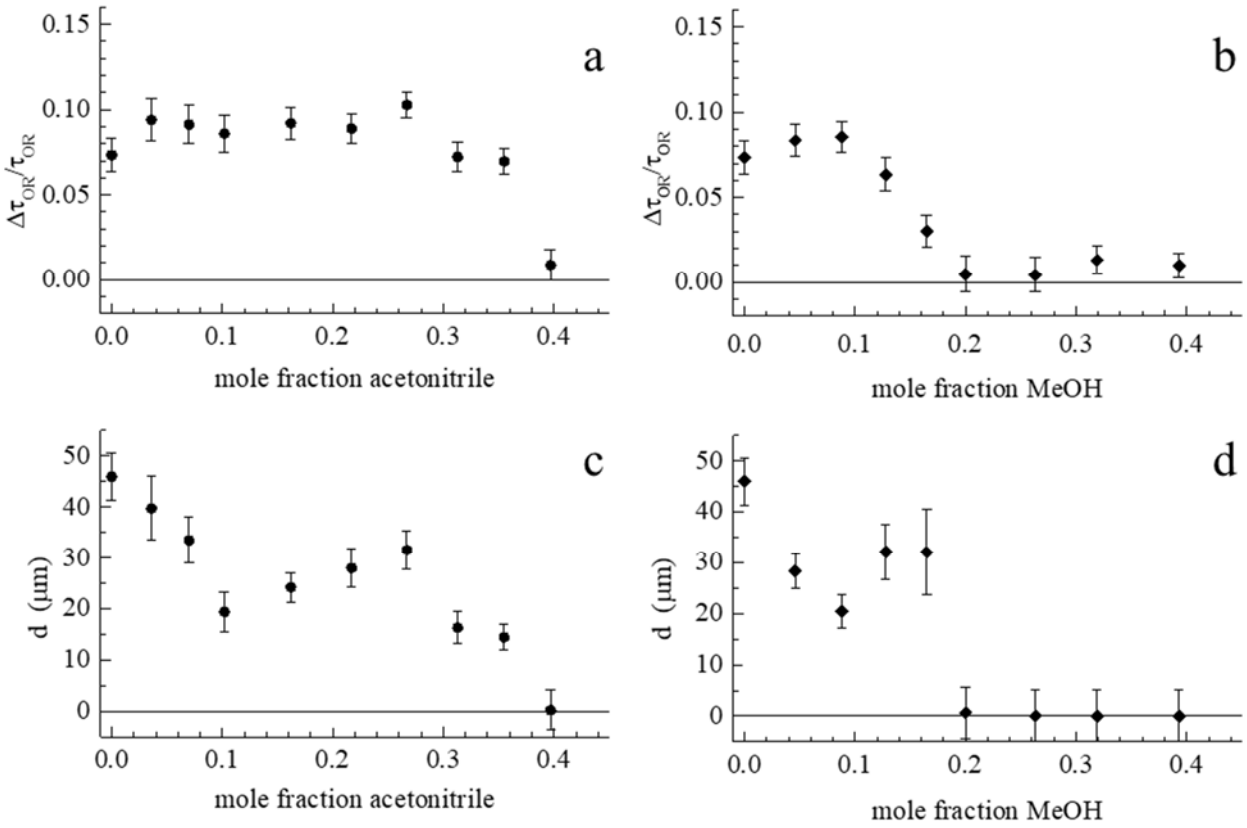

Figure 2. Dependence of magnitude of ρ_f, $(\Delta\tau_{or}/\tau_{or})(0)$, (top panels) and persistence length of ρ_f, d, (bottom panels) for $BMIM^+BF_4^-$ on dilution with acetonitrile (left panels) and methanol (right panels). Mole fractions are calculated using the associated RTIL (ion pair) and the molecular solvent.

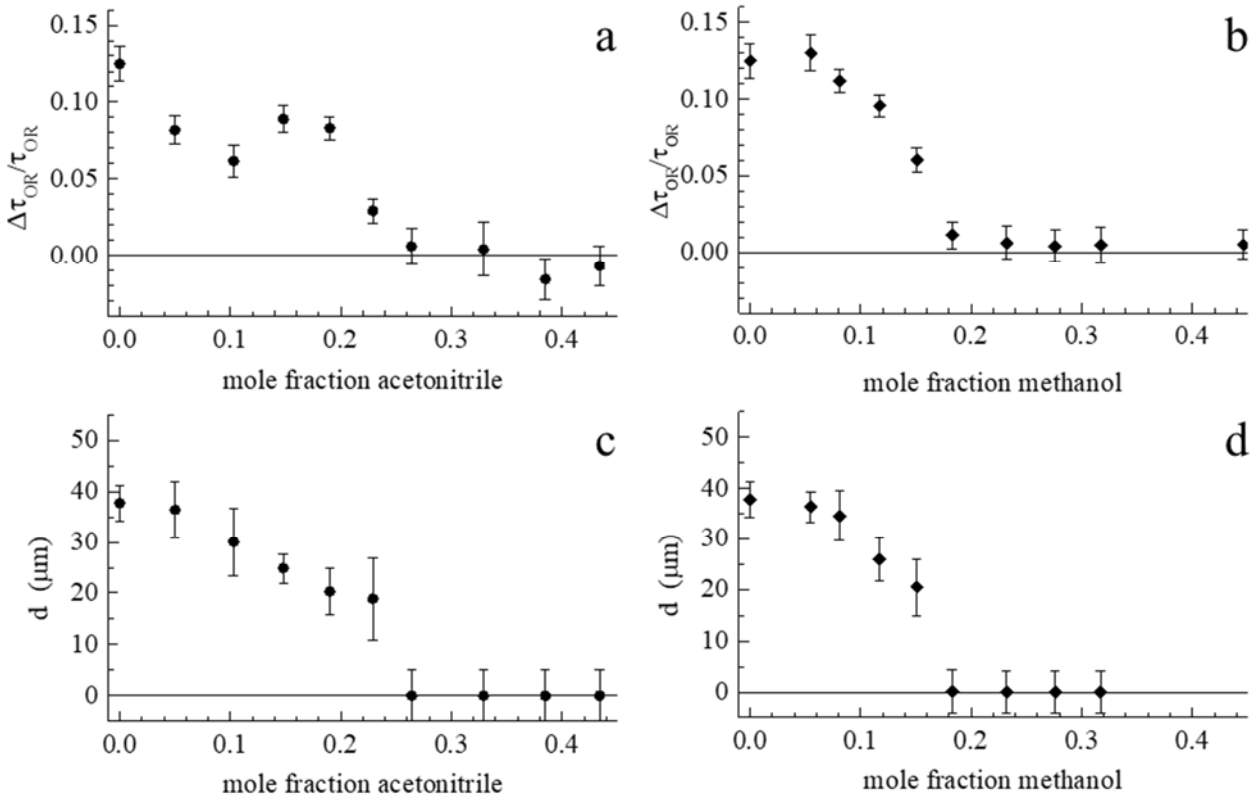

Figure 3. Dependence of magnitude of ρ_f, $(\Delta\tau_{or}/\tau_{or})(0)$, (top panels) and persistence length of ρ_f, d, (bottom panels) for $BMIM^+TFSI^-$ on dilution with acetonitrile (left panels) and methanol (right panels). Mole fractions are calculated using the associated RTIL (ion pair) and the molecular solvent.

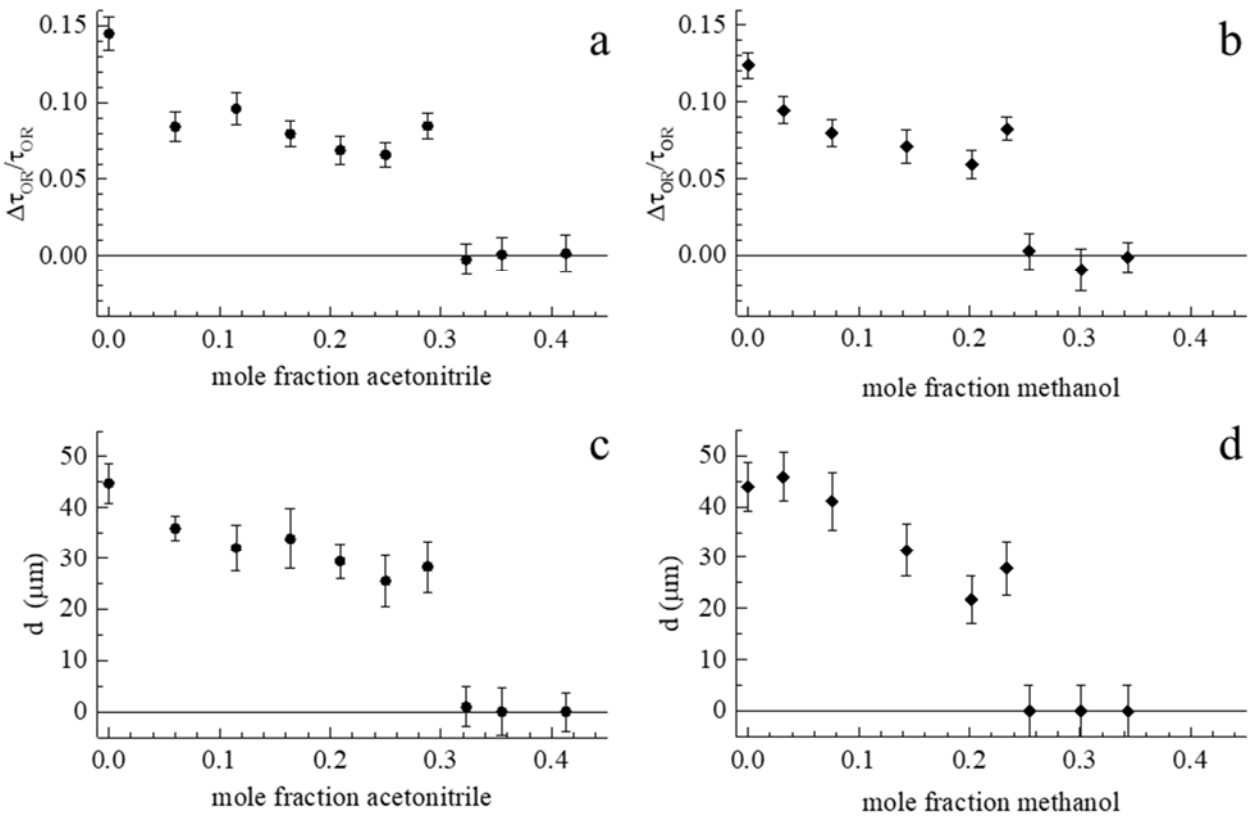

Figure 4. Dependence of magnitude of ρ_f, $(\Delta\tau_{or}/\tau_{or})(0)$, (top panels) and persistence length of ρ_f, d, (bottom panels) for $HMIM^+TFSI^-$ on dilution with acetonitrile (left panels) and methanol (right panels). Mole fractions are calculated using the associated RTIL (ion pair) and the molecular solvent.

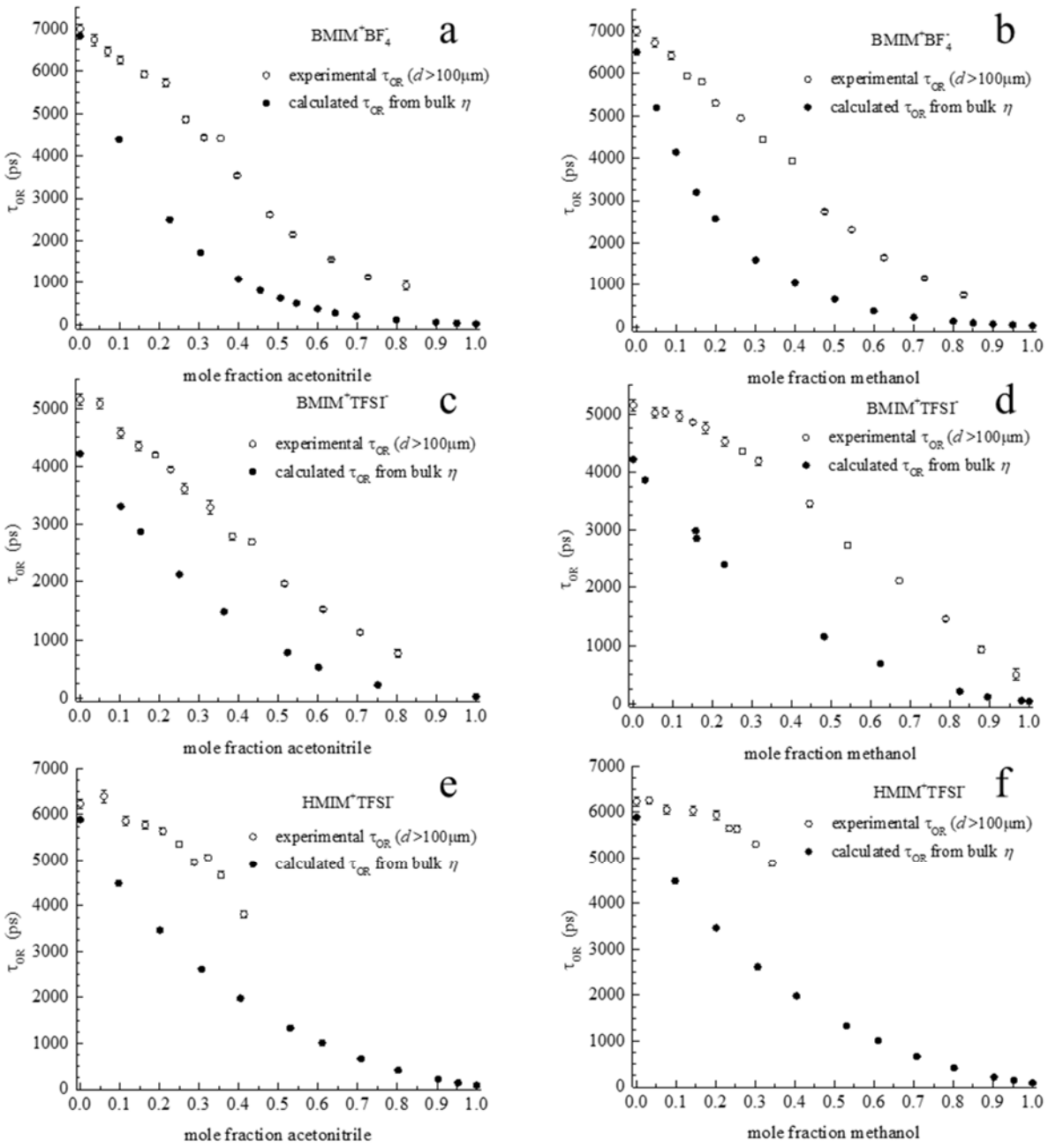

Figure 5. Reorientation time constant, τ_{OR}, observed experimentally (open circles) in bulk RTIL as a function of dilution, and calculated using Eq. 7 with reported values of the RTIL-solvent bulk viscosity (solid circles) for (a) $BMIM^+BF_4^-$ in acetonitrile, (b) $BMIM^+BF_4^-$ in methanol, (c) $BMIM^+TFSI^-$ in acetonitrile, (d) $BMIM^+TFSI^-$ in methanol, (e) $HMIM^+TFSI^-$ in acetonitrile and (f) $HMIM^+TFSI^-$ in methanol. Mole fractions are calculated using the associated RTIL (ion pair) and the molecular solvent.

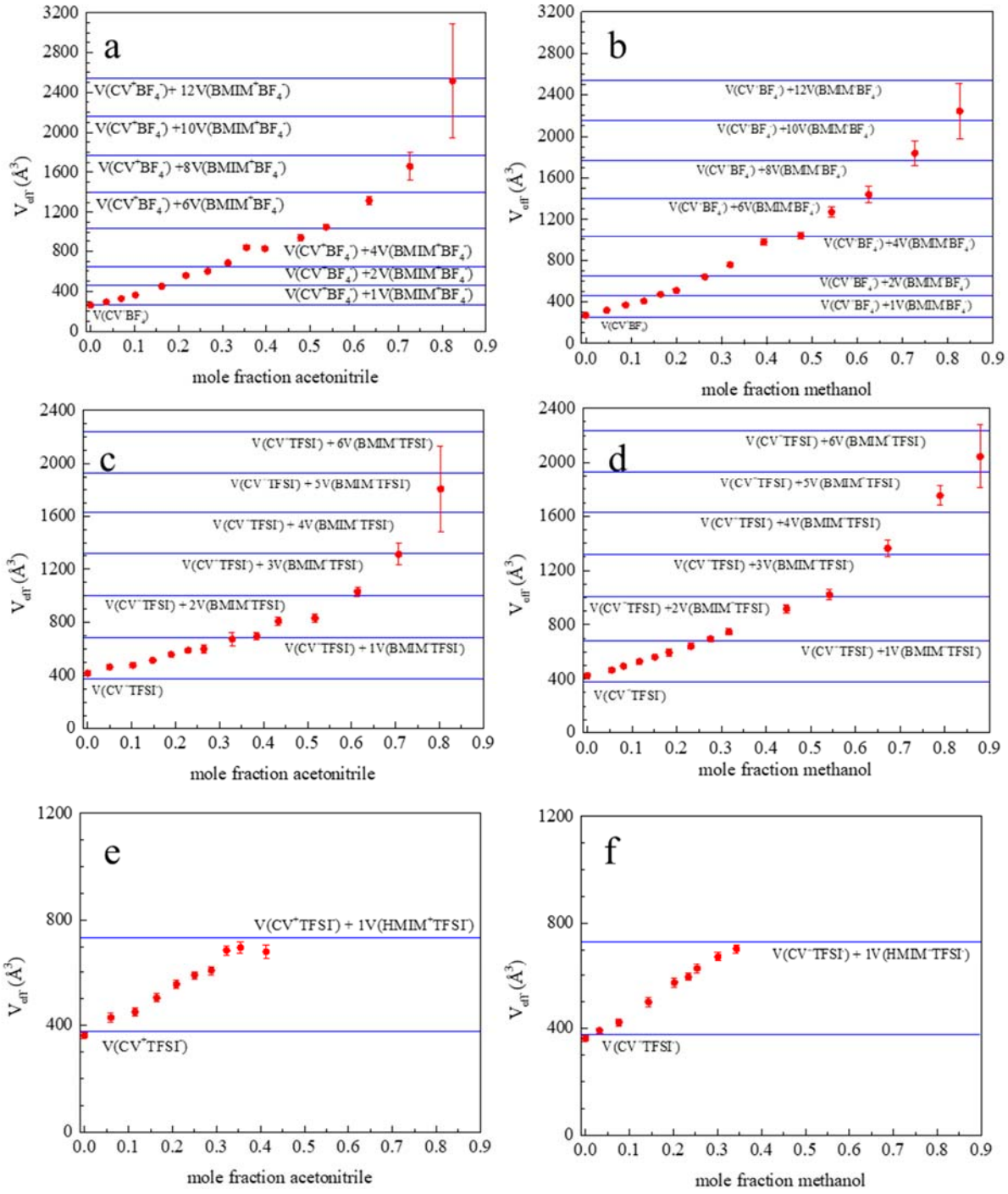

Figure 6. Effective volume, V_{eff} (red circles) of rotating entity in the RTIL-solvent binary system as a function of dilution. V_{eff} was determined from the experimental reorientation time constants, τ_{OR}, shown in Figure 5. Calculated hydrodynamic volumes of CV^+-RTIL anion with number of RTIL ion pairs indicated as blue solid lines. (a) $BMIM^+BF_4^-$ in acetonitrile, (b) $BMIM^+BF_4^-$ in methanol, (c) $BMIM^+TFSI^-$ in acetonitrile, (d) $BMIM^+TFSI^-$ in methanol, (e) $HMIM^+TFSI^-$ in acetonitrile and (f) $HMIM^+TFSI^-$ in methanol. Mole fractions are calculated using the associated RTIL (ion pair) and the molecular solvent.